Divergence reduction of laser accelerated proton beams

K. Markey, S. Kar, P. T. Simpson, B. Dromey and M. Zepf
Centre for Plasma Physics, the Queen's University, Belfast, BT7 1NN, UK

C. Bellei, S. R. Nagel, S. Kneip, Z. Najmudin and L. Willingale
Blackett Laboratory, Imperial College, London, SW7 2BZ, UK

J. S. Green, P. A. Norreys, R. J. Clarke and D. Neely
Central Laser Facility, STFC, Rutherford Appleton Laboratory, Chilton, OX11 0QX, UK

D. C. Carroll and P. McKenna
Department of Physics, University of Strathclyde, Glasgow, G4 0NG, UK

E. L. Clarke
Technological Educational Institute of Crete, Branch of Chania, Romanou 3, Chalepa, Chania, Crete, Greece 73133

K. Krushelnick
University of Michigan, Ann Arbor, MI 48109, USA

A. Schiavi
Departmento di Energetica, Universita di Roma, "La Sapienza", 00185 Roma, Italy

Main contact email address **k.markey@qub.ac.uk**

Introduction

Recent years have seen rapid growth in the area of particle acceleration from laser plasma interaction [1-6]. This development has been fueled by advances in laser design with focused intensities greater than 10^{18} W/cm^2 (the threshold for relativistic electron quiver motion) now achievable with compact systems. At this intensity regime the charge separation fields created in a plasma offer a far larger acceleration gradient (10^{12} V/m) than those achieved in conventional RF accelerator cavity structures (10^9 V/m).

Extensive worldwide investigation has revealed that proton beams accelerated from intense irradiation of thin foils possess several qualities highly desirable in applications such as proton radiography, cancer therapy, radioisotope production, compact particle acceleration and isochoric heating [7]. The target normal sheath acceleration (TNSA) of surface contaminant protons within a small emission region leads to beams with excellent longitudinal and transverse emittance [8,9], picosecond scale initial burst duration and high peak current. While these properties have been displayed in a highly consistent fashion, typical proton beams also exhibit a broad energy spectrum (100% up to E_{max}) and a large divergence angle (typically 40-60 degrees depending on laser and target parameters). These properties limit the usable proton flux for many applications which have limited angular acceptance [10] and require higher flux per unit energy than currently available.

Here we present a scheme to reduce the entire proton beam divergence while preserving the beam laminarity, yielding significant increases in peak proton flux. The scheme relies on the initial expulsion of hot electrons from a thin foil by the intense laser irradiation. Return current is drawn into the irradiated region from the surrounding material until the entire target is at an equilibrated potential. The foil is attached to a 'washer' structure through which the proton beam propagates. A transverse field similar to that of a conventional electrostatic Einzel lens is created by the resulting potential distribution. The characteristics of the washer focusing power for a range of 'washer' dimensions were investigated experimentally and verified by 3D particle tracing software.

Experiment

The experiment was carried out on the Vulcan Petawatt facility at the Rutherford Appleton Laboratory. The laser delivered ~300 J of energy to the target in a 500 fs FWHM pulse. This pulse was focused with an f/3 off axis parabola to an intensity of ~6×10^{20} W/cm^2 in an ~8 μm focal spot. Free standing 15 μm gold foils were irradiated to record typical proton beam energy spectra and energy dependent divergence. These results were compared to the case when the laser was focused on identical foils attached to cylindrical or rectangular geometry 'washers' (see Figure 1(a),(b))where the proton beam would propagate along the longitudinal axis of the 'washer'. Stacks of radiochromic film (RCF) [11,12] were used to simultaneously measure the energy spectrum and spatial profile of both the front and rear surface proton beams (Figure 1(c)). The strongly energy dependent nature of proton energy loss in matter means that the proton dose recorded on each layer of RCF corresponded predominantly to a narrow spectral energy interval. Calibration of the dose response of the RCF was done by exposing them to known proton doses in a linear accelerator [13]. The spatially integrated dose could then be converted to absolute proton numbers within the specific energy interval and the total energy spectrum inferred. In some shots, copper sheets of suitable thickness were interspersed with the RCF layers to simultaneously infer the spectrum via the proton activation method for comparison [14]. Two periodic copper meshes were inserted in the beam, imparting visible imprints in the beam due to small angle proton scattering. This allowed beam size measurements

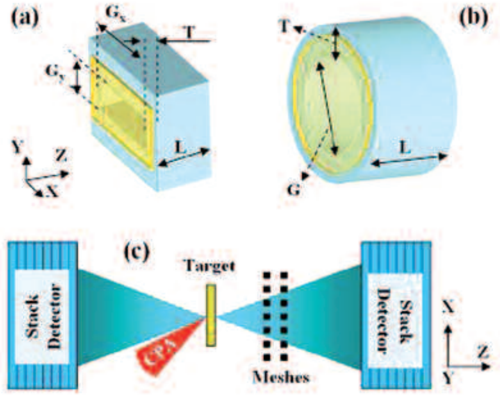

Figure 1. Schematic of (a) rectangular and (b) cylindrical 'washer' targets fielded in the experiment. (c) Schematic of the experimental setup (top view).

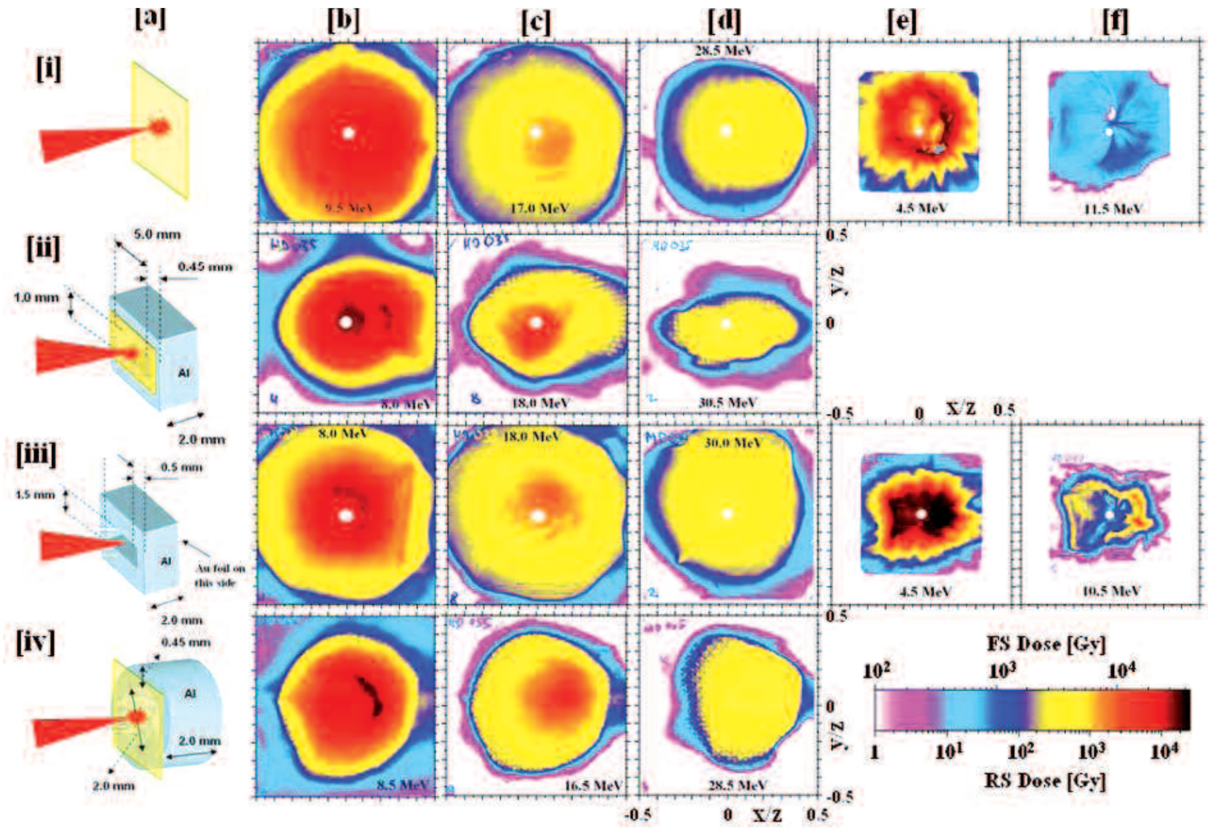

Figure 2. Experimentally obtained RCF images of proton beam profiles for four different targets illustrated in column [a]. The dominant proton energy is indicated for each RCF layer. Columns [b-d] and [e-f] consist of comparable energy layers from the rear surface and front surface stacks respectively. Measured dose is indicated by the colour scale included. Beam sizes are normalised to the RCF distance to the target.

both at the RCF plane and the two mesh planes to be measured, indicating proton trajectories, beam laminarity and virtual source position. Typical beam profiles from the experiment are displayed in Figure 2. The proton beam produced from a simple flat foil was found to be highly reproducible with an almost constant divergence angle of ~56 degrees at energies up to about 25 MeV (Figure 2[i]). The divergence at higher energies reduces as the energy cutoff is approached. The rectangular aluminium washer (Figure 2[ii]) clearly reduces the vertical beam divergence with a 2:1 vertical to horizontal divergence ratio discernable in figure 2[ii](c). When a 'washer' was mounted on the front side of the foil (Figure 2[iii]), the rear surface proton beam is almost identical to the flat foil case while the front surface beam shows clear evidence of increased peak flux from the flat foil case (Figure 2, columns (e) and (f)). When a cylindrical 'washer' beam (Figure 2[iv]) is compared to the rectangular geometry the symmetry of the focusing effect is unambiguously due to the 'washer' symmetry.

Where there is divergence reduction due to the presence of the 'washer' the dose profile recorded on the RCF indicated commensurate increases in proton flux. This result is more generally replicated in the inferred proton energy spectra where no significant (within the shot to shot and experimental error) change from the proton energy spectra of the flat foil is detected for the 'washer' targets. Moreover the energy cutoff is not affected within shot to shot variations. Reasonable agreement was found between the integrated proton dose measurement and the copper activation measurement. The mesh radiography indicated straight line particle trajectories between the two meshes. This indicated that any effect on the beam divergence takes place in the immediate vicinity of the 'washer', beyond which the proton divergence remains constant. The pronounced mesh images visible on the RCF also confirm that the 'washer' field does not destroy the beam laminarity.

Discussion

In high power laser interactions with solid targets a significant fraction of the laser energy (up to 50%[15,16]) is transferred to electrons. The total number of hot electrons can be estimated as $N_0 \sim E_L/U_p$, where E_L is the absorbed laser energy and U_p is the laser ponderomotive potential. The hot electron population has an approximately exponential energy spectrum given by $dN/dE = (N_0/U_p)\exp(-E/U_p)$ i.e. a quasi-thermal distribution with the hot electron temperature, T_e, of the order of U_p. Charging up is due to electrons which have energies greater than the target potential. The target potential evolves as a function of the intrinsic target capacitance, C_T, and escaped electron population N_{es}. For an 'infinite' flat foil, the area affected by the charge-up will expand from the initial laser spot size over the bulk of the target with a radial 'charge wave' velocity estimated at 0.75c, where c is the velocity of light[17]. The capacitance is therefore that of an expanding disk so that $C_T(t) = 8\varepsilon_0(r_0 + ct)$. The target potential represents the cutoff energy E_{cutoff} above which hot electrons can escape, so $E_{cutoff} = eN_{es}(t)/C_T$. The number of electrons in the distribution that will escape is then given by $N_{es}(t)= N_0\exp(-E_{cutoff}(t)/U_p)$. The escaped charge and target potential can be numerically calculated and, for parameters appropriate to this

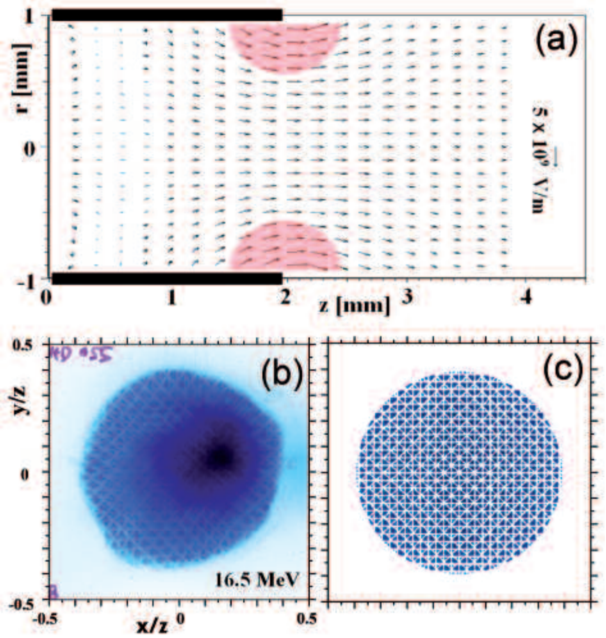

Figure 3. (a) Ptrace map of the longitudinal (across X-Z plane) electric field profile for the cylindrical 'washer' in Figure 2[iv]. Note highlighted areas of strongest focusing field. (b) Experimental and (c) simulated mesh radiographs for 16.5 MeV protons obtained from the target.

experiment, the target is maintained at megavolt potentials over the timescale relevant to proton acceleration and beam propagation through the 'washer'. At later times other effects will become important such as electron energy losses and a neutralizing current through the target mount. The targets were mounted on plastic stalks to reduce the latter effect.

3D simulations of the washer focusing were carried out using Ptrace[18]. The trajectories of test particles in the washer field were determined for a variety of washer dimensions to study their effect on the focusing power. The electric field at a given point within the washer is numerically calculated by the superposition of fields from elemental segments of the structure. The dynamic evolution of the washer field was incorporated into the cylindrical 'washer' simulations due to their simple symmetry. In the simulation the field structure reaches a steady state at a time t_{ss}, when the charge wave has traveled from the foil centre to the opening of the 'washer' i.e. $r_0 + 0.75ct_{ss} = G/2 + L$. The simulated 'steady state' field structure for the cylindrical 'washer' in Figure 2[iv] is displayed in Figure 3(a). By inputting the copper mesh positions, period and orientation, simulated RCF radiographs were generated and show good agreement with experimentally observed mesh images (figure 3(b),(c)). The simulations also show good agreement with the overall beam divergence reductions measured experimentally for different 'washer' dimensions. From figure 3(a) it is clear that the strongest focusing fields are present at the edges of the 'washer' opening. For increased focusing the most divergent protons must travel through this region indicating an optimum 'washer' aspect ratio, close to the angle at which the beam would clip the 'washer' in the absence of a focusing field. For divergent protons, the longitudinal 'washer' field will also have a focusing effect. Decreasing the 'washer' thickness, thereby reducing the total surface area should also increase the focusing effect. These trends were clearly displayed by the simulated scaling of the cylindrical washer focusing effect which was, in turn, found to compare well with experimental results (Figure 4). The rectangular washer results clearly follow the same trend at more optimized aspect ratios, where the strongest effects were recorded. The dependence of the focusing field strength on the equilibrating current drawn from the 'washer' is clearly indicated by the significant reduction in focusing power when a plastic 'washer' is used, compared to an aluminium 'washer' of identical dimensions.

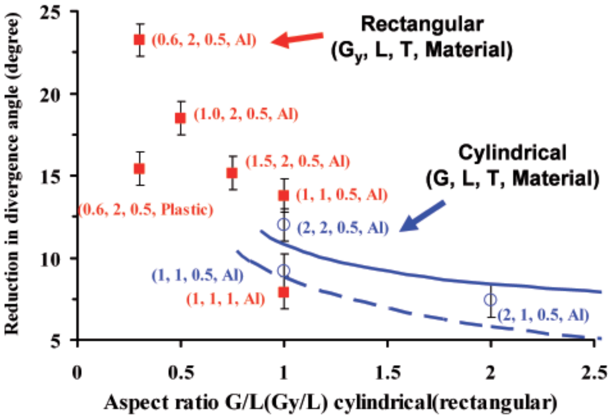

Figure 4. Experimentally obtained data points showing reduction in 17.5 MeV proton beam divergence due to rectangular (square points) and cylindrical (circular points) 'washers'. Individual target dimensions are indicated. Solid and dotted lines are simulated values for 0.5mm thick, cylindrical washers of 2 mm and 1 mm length, L, respectively.

Conclusions

We have presented experimental results of a scheme to reduce proton beam divergence from conventional flat foil targets. Charging of the target to MV potentials by the laser interaction is exploited by suitable target design to create an electrostatic lens scenario, with significant beam divergence reduction demonstrated, while preserving the beam laminarity. The focusing mechanism has been verified by 3D particle tracing simulations and key target design issues identified with regard to optimization of the scheme.

References

1. S. P. D. Mangles *et al.*, *Nature*, **431**, 535 (2004).
2. C. G. R. Geddes *et al.*, *Nature*, **431**, 538 (2004).
3. J. Faure *et al.*, *Nature*, **431**, 541 (2004).
4. E. Clark *et al.*, *Phys. Rev. Lett.*, **84**, 670 (2000).
5. R. Snavely *et al.*, *Phys. Rev. Lett.*, **85**, 2945 (2000).
6. B. M. Hegelich *et al.*, *Nature*, **439**, 441 (2006).
7. M. Borghesi *et al.*, *Fusion Sci. Tech.*, **49**, 412 (2006).
8. M. Borghesi *et al.*, *Phys. Rev. Lett.*, **92**, 55003 (2004).
9. T. E. Cowan *et al.*, *Phys. Rev. Lett.*, **92**, 204801 (2004).
10. T. Toncian *et al.*, *Science*, **312**, 410 (2006).
11. http://www.ispcorp.com/products/dosimetry/index.htm.
12. M. Borghesi *et al.*, *Phys. Plasmas*, **9**, 2214 (2002).
13. T. Toncian, Private communication.
14. P. McKenna *et al.*, *Phys. Rev. E*, **70**, 036405 (2004).
15. K.B. Wharton *et al.*, *Phys. Rev. Lett.*, **81**, 822 (1998).
16. S.C. Wilks *et al.*, *IEEE J. Quant. Electron.*, **33**, 1954 (1997).
17. P. McKenna *et al.*, *Phys. Rev. Lett.*, **98**, 145001 (2007).
18. A. Schiavi, Ph.D. Thesis, Imperial College, London, U.K. (2003).